

Received 22 May 2023, accepted 13 June 2023, date of publication 21 June 2023, date of current version 27 June 2023.

Digital Object Identifier 10.1109/ACCESS.2023.3288427

## RESEARCH ARTICLE

# Enhanced Microgrid Reliability Through Optimal Battery Energy Storage System Type and Sizing

MOHAMMADREZA GHOLAMI<sup>1</sup>, SOAD ABOKHAMIS MOUSAVI<sup>2</sup>,  
AND S. M. MUYEEN<sup>3</sup>, (Senior Member, IEEE)

<sup>1</sup>Department of Electrical and Electronic Engineering, Final International University, Kyrenia 99320, Turkey

<sup>2</sup>Faculty of Architecture and Fine Arts, Final International University, Kyrenia 99320, Turkey

<sup>3</sup>Department of Electrical Engineering, Qatar University, Doha, Qatar

Corresponding author: S. M. Muyeen (sm.muyeen@qu.edu.qa)

Open Access funding provided by the Qatar National Library.

**ABSTRACT** Reliability plays a crucial role in the design and implementation of microgrids (MGs). The integration of battery energy storage systems (BESSs) with renewable energies has been proposed as a solution to enhance reliability. However, it is important to consider the type of BESS during integration to avoid overly optimistic evaluations of reliability and cost analysis in MGs. This paper aims to address this issue by finding the optimal size and type of BESS for improving the reliability of a MG. Several factors of the BESS, such as rated power, power cost, discharge time, efficiency, and life cycle, are considered based on the type of BESS. The total electricity price and reliability indices for both grid-connected and islanded MGs are calculated, with and without considering the optimal size of the BESS. To determine the optimized size, a firefly optimization algorithm is used as an efficient meta-heuristic approach. The total cost, which includes the cost of generation units, exchanged electricity cost, and BESS investment cost, is considered as the fitness function for the problem. The results of the study show that utilizing BESS in grid-connected MGs without limitations on exchanged power with the main grid may not be economically beneficial and may not significantly improve reliability. However, it can improve the expected energy not supplied (EENS) of both islanded and grid-connected MGs with power exchange limitations by up to 10.2% and 35.77%, respectively. Additionally, life cycle is an important factor in determining the type of BESS for islanded MGs.

**INDEX TERMS** Reliability indices, microgrid, battery energy storage system, optimal size of BESS.

## I. INTRODUCTION

Microgrids (MGs) are small-scale smart power systems that play a vital role in ensuring reliable and efficient electricity supply to customers while promoting localized generation and enhancing grid resilience. MGs can be islanded or linked to the main grid [1], [2]. MGs bring many benefits to emission mitigation and to the power system performance in term of control, monitoring, and flexibility. In spite of all these advantages, the reliability of a MG has been always a challenge. Due to uncertainties and dependency to weather condition in output power of renewable energies and load demand [3],

The associate editor coordinating the review of this manuscript and approving it for publication was Ahmed Mohamed<sup>id</sup>.

improving the reliability of MGs has attracted the attention of many researchers in this area. Battery Energy storage systems (BESSs) are one of the most effective technologies used to improve the reliability of MGs [4]. BESSs are charged during low-price electricity hours and discharged during peak hours which the price of electricity is high [4], [5], [6]. Also, they can provide energy to cover fluctuation in load demand, and in emergency cases and when there is an interruption in power delivery in the power system [7], [8]. Utilizing BESSs are associated with other benefits such as increasing power quality and voltage and frequency stability [9], [10].

The main objective considered in using an BESS in a MG is to find the optimized size of the BESS in which the total cost is minimized [11]. The total cost mostly includes

production and maintenance of generation, investment and maintenance of BESS, and cost of exchanging the power between MG and main grid. Obviously, by utilizing oversized BESS, the investment cost and consequently the total cost is increased. At the same time decreasing the size of the BESS has negative effects on MG performance, power quality and reliability [12]. Various methods are applied to find the optimal size of the BESS from mixed integer linear and nonlinear programming [13] and dynamic programming [14] to particle swarm optimization algorithm as a metaheuristic method [15]. In [16] and [17] the uncertainty is considered and probabilistic optimization model is used for optimal sizing of the BESS. The effect of the utilizing the optimum size of the BESS in MG reliability is not addressed in these researches or just discussed qualitatively.

In [18], the authors calculate the reliability indices considering mobile BESS. They evaluated reliability in presence of BESS integrated with renewable energies. Also, they proposed a developing a Markov based model of BESS. They applied Monte Carlo simulation (MCS) for reliability evaluation. Their results show that renewable energies have improved the reliability by 5 percent without BESS and up to 36 percent considering 5MWh BESS integrated with renewable energies. However, they just considered fixed size, 500 KWh, 1MWh, 2MWh, and 5MWh, for BESS in their study. The optimized size of BESS is not addressed in their study.

In [19] the effect of utilizing battery ESS (BESS) on reliability of a MG is well addressed quantitatively. The authors first determined an optimal size of the BESS considering minimum total cost using a mixed integer linear programming. Then the reliability indices are calculated with and without utilizing BESS. Their results show the significant effect of BESS on all reliability indices and minimizing the total cost at the same time. However, they considered fixed values for parameters such as, rated power and energy cost of BESS, and rate and cost of the exchanged power with the main grid. They briefly explain different types of BESSs, but the effect of type of the BESS in the reliability is not evaluated in their study. In addition, the price of exchanged power with the main grid is considered as a fix price and independent from the time of the day.

ESSs are classified into various technologies based on the types of energy they consume such as mechanical, chemical, electrical, thermal and electrochemical. Pumped hydro storage (PHS) [20], compressed air energy storage (CAES) [21] and flywheel energy storage (FES) [22] are different mechanical based technologies. Superconducting magnetic energy storage (SMES) [23] and super-capacitor energy storage [24] are electrical based types of ESS. Electrochemical types include wide range of technologies such as Lead–Acid Battery (LA), Nickel–Cadmium and Nickel–Metal Hydride Battery (NiCd, NiMH), Lithium-Ion Battery (Li-Ion), Metal–Air Battery, Sodium–Sulphur Battery (NaS), Redox Flow Battery (RFB), and Hybrid Flow Battery (HFB). More details regarding operation and features

of these types can be found in [25], [26], and [27]. BESS technologies exhibit different technical specifications and limitations, including power rating, power and energy cost rates, efficiency, discharge time, and lifetime.

This paper addresses a research gap and extends the investigation related to the optimal size of BESS in [19]. By considering the interplay of BESS type, time-varying exchanged power prices, and the specific characteristics of different MG types, we aim to provide valuable insights into the reliability enhancement potential of BESS in diverse MG settings in the following ways:

- Considers the type of BESS in reliability power system analysis: The effect of different BESS types and related parameters on MG reliability is evaluated. By considering the type of BESS and its associated characteristics in the optimal sizing process and reliability analysis of the MG, we ensure that the results are realistic and avoid overly optimistic evaluations. Neglecting considering the BESS type can lead to unrealistic outcomes and misleading conclusions. Therefore, it is crucial to consider the practical limitations and constraints such as efficiency, price, rated limitation, and failure rate, to obtain reliable and accurate results in both the optimal sizing and reliability assessment of the MG.

- Incorporates time-varying exchanged power prices: One significant economic advantage of utilizing BESSs in MG is the ability to charge BESSs during low-price electricity hours and discharge during high-price hours to shave peak demand. This paper addresses this advantage by considering exchanged power price as a time-varying variable.

- Considers different MG types and scenarios: To conduct a more accurate economic analysis and evaluate the effect of utilizing BESS in MG reliability, this paper considers the MG type as grid-connected and islanded, as well as two scenarios with and without limitations in exchanged power with the main grid for the grid-connected MG.

The remainder of the paper is organized as follows. Section II presents the methodology used in the study including the flowchart of the utilized approach. The mathematical formulation of the problem, including the optimal sizing of an ESS, the assessment of reliability indices, and the application of firefly algorithm (FA) to find the optimal solution are provided in Section III. In Section IV, we provide information on the case study and data related to different types of BESS, along with the results achieved by applying the optimization algorithm. Section V discusses the results and data of the various BESS types, providing a detailed analysis and comparison. Finally, in Section VI, we present our conclusion, summarizing the main contributions of the paper and highlighting areas for future research.

## II. METHODOLOGY

In this section, we present the methodology employed in this study. The methodology and approach is divided into three parts: Input data, optimal sizing of BESS, and reliability indices assessment. The input data used in this analysis include load profile which represents the electricity demand

pattern of the MG over a specific time period; RES data consists of installed capacity of the RES and output power distribution during time period, and reliability data such as failure rates and repair times for the different components. Also, different BESS types data considering their limitations and characteristics such as energy capacity, power rating, charging / discharging efficiency values, and state of charge limits are fed into the input data. In addition, the base attractiveness, gamma value, step size, and termination conditions are the input data set to control the FA operation.

The steps of the utilized approach are provided as follows:

- First, input data including load profile, RESSs, BESS different type's data, components' reliability data, and FA initial parameters.

- Second, select the scenario (islanded MG, grid-connected MG with exchanged power limitation, and grid-connected MG without exchanged power limitation with the main grid)

- Third, run the FA until the maximum number of iterations is reached:

The first population of fireflies is generated randomly. Each firefly represents a possible solution of the problem including the type of BESS, size of BESS, and BESS statuses for 24 hours a day.

The fitness function for each firefly is evaluated (which is total cost of the MG considering the optimal size of BESS and the selected type of BESS).

The fireflies are moved toward new positions.

The total cost of MG is reevaluated for improved fireflies.

- Finally, calculate the reliability indices based on the best solution found.

Our innovation lies in updating the formulation for determining the optimal size of the BESS while considering the limitations and characteristics of different BESS types. Varying parameters for the BESS based on its type, including the maximum rated power, life cycles, and charging and discharging efficiencies are considered in finding the optimal size of BESS. By integrating these factors into the sizing formula, we aim to achieve more accurate and tailored results for the optimal BESS capacity required to meet the MG demand and enhance its overall performance. Additionally, an analysis of the effect of different BESS types on both islanded and grid-connected MG, with and without power exchange limitation with the main grid, configurations is conducted.

### III. PROBLEM FORMULATION

This section consists of description and formulation of optimal sizing of an ESS, reliability assessment of the MG, and applied particle swarm optimization algorithms:

#### A. OPTIMAL SIZING OF AN ESS

An Oversized BESS leads to higher unnecessary investment cost in the grid, while, an undersized BESS may not be able to supply sufficient load and bring economic and technical benefits. The main goal of the optimal ESS sizing is to find the optimized size of BESS to minimize the total cost of

the grid. The total cost includes the costs related to generation unit's cost, cost of the exchanged electricity with the main grid and the BESS investment cost for a given horizon time (1).

$$\min TC = MGC_{units} + MGC_{exchanged} + IC_{ESS} \quad (1)$$

where  $TC$  represents the total cost of the MG should be minimized.  $MGC_{units}$ ,  $MGC_{exchange}$ , and  $IC_{ESS}$  are the cost of generation units, exchanged power of MG with the main grid, and investment cost of the BESS respectively which can be calculated using equations (2-4).

$$MGC_{units} = \sum_{t=1}^{NT} \sum_{i=1}^{NI} FC_i \alpha_{i,t} + VC_i P_{i,t} + SU_i \beta_{i,t} + SD_i \gamma_{i,t} + MC_{i,t} \quad (2)$$

where,  $NT$  and  $NI$  are the number of times and units.  $FC_i$ ,  $VC_i$ ,  $SU_i$ , and  $SD_i$  are represent the fixed, variable, startup, and shutdown cost of  $i_{th}$  unit respectively.  $P_{i,t}$  is the power of unit  $i$  at time  $t$ . Also,  $\alpha_{i,t}$ ,  $\beta_{i,t}$ , and  $\gamma_{i,t}$  are binary variables indicate the statues of  $i_{th}$  unit in MG at the time  $t$ . Also,  $MC_{i,t}$  represents the maintenance cost of generation unit  $i$  at time  $t$  which is calculated using equation (3):

$$MC_{i,t} = k_{cmi,t} P_{i,t} \quad (3)$$

where,  $k_{cmi,t}$  is the maintenance cost coefficients per 1 kWh of generation unit  $i$ .

$$MGC_{exchanged} = \sum_{t=1}^{NT} \rho_{i,t} \times EP_t \quad (4)$$

where,  $EP_t$  is the exchanged power at time  $t$ . Also,  $\rho_{it}$  is price of the 1 KWh of power bought from or sold to the main grid at time  $t$ . This price is considered as a variable in this study vary based on the time of the day.

$$IC_{ESS} = PC_{ESS} \times P_{rated_{ESS}} + EC_{ESS} \times E_{rated_{ESS}} + OC_{BESS} + MC_{BESS} \quad (5)$$

where,  $PC_{ESS}$  and  $EC_{ESS}$  are power and energy cost of ESS per KW and KWh respectively. Also,  $P_{rated_{ESS}}$  and  $E_{rated_{ESS}}$  represent rated power and energy of ESS which are variables of this problem.

Also,  $OC_{BESS}$  and  $MC_{BESS}$  are the operation and maintenance cost of BESS, calculated using equations (6) and (7) respectively:

$$OC_{BESS} = \sum_{t=1}^{NT} CC(t) + \frac{RC_{BESS}}{LT_{BESS}} \quad (6)$$

$$MC_{BESS} = \sum_{t=1}^{NT} k_{cmBESS} P_{BESS,t} \quad (7)$$

where,  $CC(t)$  is the cost of charging the BESS based on the charging source. The  $RE_{BESS}$  and  $LT_{BESS}$  are the replacement cost and total lifetime (life cycles) of the BESS. Also,  $k_{cmBESS}$  is the maintenance cost coefficients per 1 kWh of BESS.

In this study, the optimal type and size of the BESS are determined based on minimizing the total cost of the MG, which includes factors such as initial investment, maintenance cost, and any associated operational expenses. By considering the lifetime of the BESS and its corresponding operational cost, we can optimize the selection and sizing of the BESS to achieve the most cost-effective and reliable MG configuration. Obviously, higher life time leads to a lower operational cost of BESS.

$$\sum_{i=1}^{NI} EP_t + P_{rated_{ESS}} + P_{i,t} = Load_t \quad \forall t \in NT \quad (8)$$

Regarding the equation (8), the power of BESS is considered as a load, with negative sign in the equation, when it is charged by generation units. Similarly, the exchanged power is considered negative and positive when the power is exported and imported from main grid respectively.

### B. MODELLING OF SYSTEM AND CONSTRAINT OF THE PROBLEM

The ESS is modeled using its constraints. Also, the constraint related to the generation units operation and transmission system is provided. Regarding the BESS, the energy stored in BESS at time t is calculated by equation (9).

$$E_{ESS,t} = E_{ESS,t-1} + (P_{ESS}^c \eta_c - \frac{P_{ESS}^d}{\eta_d}) \times \Delta t \quad \forall t \in NT \quad (9)$$

where,  $P_{BESS}^c$  and  $P_{BESS}^d$  are the ESS charging and discharging power respectively.  $\eta_c$  and  $\eta_d$  are the efficiency of charging and discharging which are vary based on type the ESS.

Also, the BESS state of charge (SoC), refers to the level of charge stored in the battery at a specific point in time, is an essential parameter that can significantly impact the performance of BESS. The SoC factor is modeled using equations (10) and (11). A higher BESS SoC allows for more energy to be stored, resulting in increased energy availability. Conversely, a lower BESS SoC may lead to a reduced energy reserve, potentially impacting the reliability of the MG during critical situations.

$$SoC_{min} \leq SoC(t) \leq SoC_{max} \quad (10)$$

$$SoC(t) = SoC(t-1) + \begin{cases} DC_b(t) & P(t) > 0 \\ CC_b(t) & P(t) < 0 \end{cases} \quad (11)$$

where, the  $SoC(t)$  indicates its current charge level, while  $SoC_{max}$  represents the maximum charge rate and  $SoC_{min}$  represents the minimum charge rate.  $DC_b$  denotes the battery's discharge consumption, and  $CC_b$  represents its charge consumption. Also,  $P(t)$  is the output power of the BESS.

Equations (12) and (13) represent that the power and energy of ESS are limited by their rated values which are determined based on the type of the ESS.

$$-P_{ESS}^R \leq P_{ESS,t} \leq P_{ESS}^R \quad \forall t \in NT \quad (12)$$

$$0 \leq E_{ESS,t} \leq E_{ESS}^R \quad \forall t \in NT \quad (13)$$

The energy stored in the BESS,  $E_{ESS,t}$  is always positive, while the power of the BESS is considered negative when it is charged.

It should be noticed that, in this study, parameters related to the BESS such as  $k_{cmBESS}$ ,  $RC_{BESS}$ ,  $LT_{BESS}$ ,  $P_{BESS}^R$ , and charging and discharging efficiencies are varying and determined based on type of the BESS.

The generation unit constraints are formulated in equations (14) to (18). The Equation (14) is related to the output power of the units which is limited by maximum power,  $P_i^{max}$ , can be generated by each unit. Also, the output power is multiplying by the binary status variable,  $u_{i,t}$ , since if the unit is OFF, then the output power is zero.

$$P_i^{min} \alpha_{i,t} \leq P_{i,t} \leq P_i^{max} \alpha_{i,t} \quad \forall t \in NT \quad \forall i \in NI \quad (14)$$

Practically, increasing and decreasing the output power of generation units is limited by the ramp up and ramp down rates which are represented by  $RU_i$  and  $RD_i$  in equations (15) and (16) respectively.

$$P_{i,t} - P_{i,t-1} \leq RU_i \quad \forall t \in NT \quad \forall i \in NI \quad (15)$$

$$P_{i,t-1} - P_{i,t} \leq RD_i \quad \forall t \in NT \quad \forall i \in NI \quad (16)$$

Also, another limitation regarding the generation units is the minimum time the unit required to be ON when it shuts down and be OFF when it starts up. These constraints are formulated in equations (17) and (18).

$$T_{i,t}^{ON} \geq MUT_i \times [\alpha_{i,t} - \alpha_{i,t-1}] \quad \forall t \in NT \quad \forall i \in NI \quad (17)$$

$$T_{i,t}^{OFF} \geq MDT_i \times [\alpha_{i,t} - \alpha_{i,t-1}] \quad \forall t \in NT \quad \forall i \in NI \quad (18)$$

where,  $MUT_i$  and  $MDT_i$  are the minimum up time and down time of the unit  $i$ . Also,  $T_{i,t}^{ON}$  and  $T_{i,t}^{OFF}$  represent the ON time and OFF time of the unit  $i$  respectively.

The last constraint regarding generation units is a logic constrain. The equation (19) guarantees that the generation units cannot shut down or start up at the same time.

$$[\beta_{i,t} - \gamma_{i,t-1}] = [\alpha_{i,t} - \alpha_{i,t-1}] \quad \forall t \in NT \quad \forall i \in NI \quad (19)$$

In addition, the limitation of the transmission lines is formulated in equation (20). The exchanged power between microgrid and the main grid is limited by the maximum capacity of the connected transmission lines.

$$0 \leq P_t^{max} \leq P_{exchanged}^{max} \quad \forall t \in NT \quad (20)$$

where,  $P_t^{max}$  is the maximum capacity of the transmission line connecting MG to the main grid.

### C. RELIABILITY ASSESSMENT

The two-state reliability model is used for the ESS and power components. The availability and unavailability of the components are calculated based on their failure rate,  $\lambda_i$ , and repair rate,  $\mu_i$ , formulated in equations (21) and (22) respectively.

$$A_i = \frac{\mu_i}{\lambda_i + \mu_i} \quad (21)$$

$$U_i = \frac{\lambda_i}{\lambda_i + \mu_i} \quad (22)$$

where  $A_i$  and  $U_i$  represents the availability and unavailability of element  $i$ . please be noted that the failure and repair rates of the BESS vary based on its type.

Since the ESS is considered to be connected to the generation units in parallel, the unavailability and availability of total system,  $U_{sys}$  and  $A_{sys}$  are calculated based on equations (23) and (24) respectively.

$$U_{sys} = \prod_{i=1}^{nc} U_i = U_{MG} \times U_{BESS} \times U_{PV} \times U_{WT} \times U_{DE} \quad (23)$$

$$A_{sys} = 1 - U_{sys} \quad (24)$$

where  $nc$  is the total number of components in the system.

In equation (23), the availability of the MG is dependent on the availability of its components such as main grid ( $U_{MG}$ ), BESS ( $U_{BESS}$ ), PV ( $U_{PV}$ ), WT ( $U_{WT}$ ), and DE ( $U_{DE}$ ), which are calculated based on the failure rate and repair time of each component. Since the failure rate of BESS is significantly lower compared to other system components, the inclusion of BESS improves the reliability indices.

The loss of load expectation (LOLE) and expected energy not supplied (EENS) are considered as reliability indices calculated using equations (25) to (28) as follows:

$$LOLP(L_i) = \sum_{i=1}^{n_f} p_i \quad (25)$$

$$P_i = \prod_{j=1}^{nc} pc_j \quad (26)$$

where  $n_f$  is the number of system failure states in which the total generation capacity is less than load demand.  $p_i$  is the probability of  $i_{th}$  state of the system.  $nc$  is the number of components in the system (generation units in our study).  $pc_j$ , the probability of component  $j$ , is equal to availability and unavailability of the component if its status is ON or OFF respectively.

LOLE in hours is calculated as sum of the loss of load probability,  $LOLP(L_i)$ , of each load in duration time (T).

$$LOLE = \sum_{i=1}^T LOLP(L_i) \quad (27)$$

$$EENS = \sum_{i=1}^T LOLP(L_i) \times r_i \quad (28)$$

EENS in KWh for the time duration is calculated based on  $LOLP(L_i)$  and the amount of demand not supplied in each load  $r_i$ .

According to the equations (25) and (26), the reliability indices are calculated based on the failure states of the system in which the total generated power is less than load demand. The utilization of BESS provides MG owners with increased flexibility and availability of energy sources, especially during peak hours and in cases of islanded MG or grid-connected MG with limitations in exchanged power with the grid. By integrating BESS into the MG system, energy

storage allows for optimal utilization of renewable energy sources and efficient load management, thereby enhancing the overall reliability of the MG.

#### D. FIREFLY ALGORITHM

One metaheuristic algorithm that has gained attention recently due to its simplicity and ease of application is the Firefly Algorithm (FA). FA is inspired by the behavior of fireflies in their natural environment, where fireflies use the intensity of their flashing lights to attract and communicate with each other. The basic steps and principles of the Firefly Algorithm are as follows:

- Initially, populations of fireflies are generated randomly in which each firefly represents a potential solution to the optimization problem.

- Then, all fireflies in the population are evaluated based on the fitness or objective function value which is the total cost of the MG in this study.

- Next step, the new and improved fireflies are created in a iteration based process using the following steps:

- Attraction: The attractiveness between fireflies is determined based on their fitness values. Brighter fireflies (higher fitness) have higher attractiveness and tend to attract dimmer fireflies (lower fitness) towards them. The attractiveness of each firefly is Calculated based on its brightness using equation (29)

$$\beta = \beta_0 \times e^{-\gamma d^2} \quad (29)$$

where  $\beta_0$  is the base value of attractiveness determines the overall attractiveness level and  $\gamma$  Controls the light absorption and affects the rate of attractiveness decrease with distance. Also,  $d^2$  is the Euclidean distance between two fireflies.

- Movement: Each firefly adjusts its position based on the attractiveness of other fireflies. Fireflies move towards brighter fireflies in a random manner, with the brightness difference and distance between fireflies influencing the movement using equation (30).

$$X_i^{t+1} = X_i^t + \beta^{-\gamma d_{ij}^2} (X_j^t - X_i^t) + \alpha_t \varepsilon_t \quad (30)$$

where  $\alpha_t$  is the step size parameter determines the step size of movement, and  $\varepsilon_t$  is the random vector calculated based on a Gaussian distribution used to introduce randomness into the movement and exploration process.

Update: After the movements, the fitness of the fireflies based on their new positions are evaluated.

Termination: Repeat steps above until a termination condition is met (a maximum number of iterations is considered in this study as the termination condition).

Regarding the control parameters, the value of  $\beta_0$  typically falls within the range of 0.1 to 1.0 which determines the overall attractiveness level among fireflies. A higher value leads to stronger attraction between fireflies. Also,  $\gamma$  is a parameter controlling the light absorption in the attractiveness calculation. It typically ranges from 0.1 to 10.0. A higher

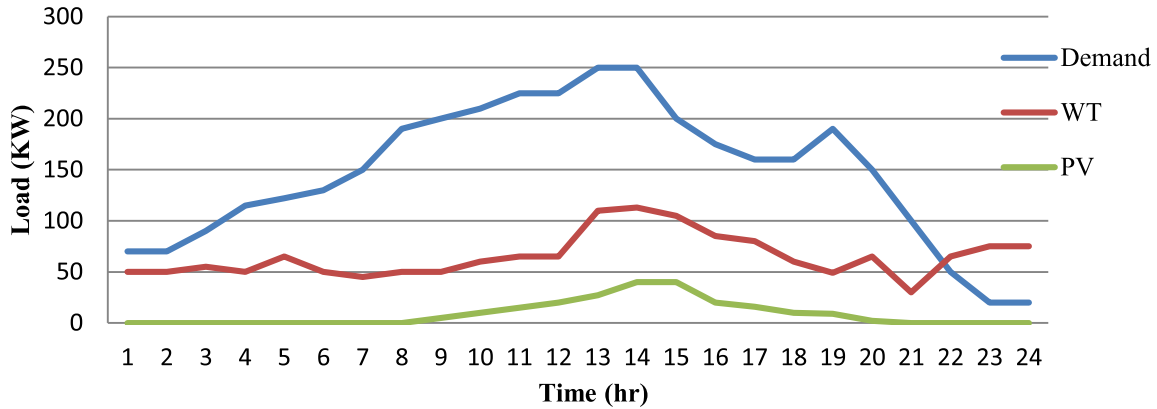


FIGURE 1. Load demand, WT output power, and PV out power data for a MG in 24 hours.

TABLE 1. DE generation unit data.

Parameter	$P_{min}$ (kW)	$P_{max}$ (kW)	Fixed cost (\$)	Variable cost (\$/kW)	Startup cost (\$)	Shutdown cost (\$)	Ramp-down rate	Ramp-up rate	Minimum downtime (h)	Minimum uptime (h)	Maintenance cost factor (\$/KWh)
DE	5	80	1.9250	0.2455	0.3	0.1	50	50	1	1	0.01258

$\gamma$  value causes the attractiveness to decrease more rapidly with distance. Finally, a typical range for  $\alpha_t$  is 0.01 to 0.1. Smaller values result in finer-grained movements.

IV. CASE STUDY AND RESULTS

In this section, the information regarding generation units and load profile of the MG under study and the data related to the different types of ESS is provided. Regarding the load demand profile, output of photovoltaic (PV) and wind turbine (WT), we used the data of the MG studied in [28]. We considered a diesel engine (DE) as controllable generation unit in the MG. Fig. 1 shows the load demand profile and output power of the PV and WT in the case study in 24 hours time with each interval of 1 hour. As it is shown, the load demand at the 12:00 am is 60 KW and is increased to 250 KW at 12:00 pm. then it drops slightly until 6:00 pm where there is an increasing in load demand. The demand is decreased significantly to 20 KW at 23:00 pm. Through all period, the WT output power is fluctuating between 50 and 115 KW. Also, the PV output power is available between 9:00 am to 8:00 pm whit maximum 40 KW at 1:00 pm. We considered the cost of energy produced by PV and WT as 0.048 (\$/kWh) and 0.033 (\$/kWh) respectively. Also, the price of electricity trading with main grid is considered 0.43, 0.3, and 0.12 (\$/kWh) in peak, intermediate and off-peak demand hours respectively.

The DE generation unit data is given in Table 1. The technical information for different types of the BESS such as power rating, efficiency, power and energy cost per KWh and life cycles are given in Table 2. In addition regarding the FA parameters,  $\beta_0$ ,  $\gamma$ , and  $\alpha_t$ , are considered 0.5, 5, and 0.05 respectively. The number of fireflies in each population and number of total iterations are set to 100 and 1000 respectively.

We considered three different scenarios in this study. In the first and second scenarios, the MG is a grid-connected MG which is connected to the main grid and it is possible to sell power to main grid or buy from it based on defined prices. However, we considered that there is a limitation in power exchange with the main grid in first scenario and no limitation in the second one. In the third scenario we assumed the MG as an islanded MG in which MG operates independently of the main grid and the demand should be supplied by renewable energies, DE, and BESS.

The Table 3, 4, and 5 show the status of DE and BESS as the best answer found by FA in scenario one, two, and three respectively. The values 1 and -1 are used to represent the status of discharging and charging of the BESS.

In the first scenario, the MG is connected to the grid and BESS can be charged using main grid. The maximum exchanged power with the main grid is considered as 100 KWh. The results of the results show that in a grid-connected MG, the BESS is mostly charged during off-peak hours and discharged during peak hours. Also, the frequency of charging and discharging of BESS in islanded MG is higher than grid-connected MG which shows that the BESS types with more life cycle should be utilized in this type of MGs. The output powers of exchanged power with the main grid, DE, and BESS for each scenario are shown in Figures 2, 3, and 4. The negative values for BESS shows the charging hours of the BESS. In first and second scenarios, grid-connected MG with and without limitation in exchanged power rate, the load demand is mostly supplied by the main grid in off-peak hours. In peak hours, it is suggested to supply the demand by the BESS and DE. Also, in case of no limitation in exchanged power with the main grid, the proportion of the main grid in supplying the load is higher than the other sources. Regarding the islanded

**TABLE 2.** Comparison of bess technologies in term of rated power and energy, efficiency, and cost [25], [29], [30].

BESS Technology	Max. Power rate	power cost (\$/KW)	Cost of electricity (\$/KWh)	Efficiency (%)	Life cycles
Lead-acid	10 KW - 100 MW	300-600	0.37	80-90	300-700
Nickel-Cadmium NiCd	40 MW	500-1500	0.94	70-90	500-1500
Nickel-Metal Hydride NiMH	40 MW	500-1500	0.56	70-90	500-1000
Li-Ion	100 MW	1200-4000	0.50	85-95	500-5000
Sodium-Sulfur (NaS)	8 MW	1000-3000	0.75	70-95	2000-4500
Metal-air	10 KW	100-250	0.3	50	500-3000
RFB / HFB	100 MW	700-2500	0.63	60-85	12000-14000

**TABLE 3.** The on-off status of DE and BESS during the day- first scenario.

Period	1	2	3	4	5	6	7	8	9	10	11	12
DE	0	0	0	0	0	0	1	1	1	1	1	1
BESS	-1	-1	-1	-1	-1	-1	0	1	1	1	1	1
Period	13	14	15	16	17	18	19	20	21	22	23	24
DE	1	1	1	0	0	0	1	0	0	0	0	0
BESS	1	1	1	0	0	0	1	0	0	-1	-1	-1

**TABLE 4.** The on-off status of DE and BESS during the day- second scenario.

Period	1	2	3	4	5	6	7	8	9	10	11	12
DE	0	0	0	0	0	0	0	0	1	1	1	1
BESS	-1	-1	-1	-1	0	0	0	0	1	1	1	1
Period	13	14	15	16	17	18	19	20	21	22	23	24
DE	1	1	1	0	0	0	0	0	0	0	0	0
BESS	1	1	1	0	0	0	0	0	0	-1	-1	-1

**TABLE 5.** The on-off status of DE and BESS during the day- third scenario.

Period	1	2	3	4	5	6	7	8	9	10	11	12
DE	0	0	1	1	1	1	1	1	1	1	1	1
BESS	1	1	-1	-1	-1	-1	1	1	1	1	1	1
Period	13	14	15	16	17	18	19	20	21	22	23	24
DE	1	1	1	1	1	1	1	1	1	0	0	0
BESS	1	1	0	0	0	0	1	-1	-1	-1	-1	-1

**TABLE 6.** Failure rate and repair rate for system components [31].

System Component	Main grid	PV	WT	DE	BESS
Failure Rate (Failure/year)	0.25	0.5	0.769	1.168	0.172
Repair Time (h)	48	40	279	100	7.8

MG, the energy supplied by BESS is remarkably higher in peak hours.

The considered values of failure and repair rates in this study for the main grid, PV, WT, DE, and BESS are provided in Table 6. Table 7 provide comparison of total cost and calculated reliability indices with and without considering the

BESS. Regarding the first and second scenarios a 23 KW Lead-acid battery, with the rated energy of 258 KWh and 202KWh, is the suggested type of BESS. Both electricity cost (by 8.06%) and reliability (by 56.2% and 35.77% for LOLE and EENS respectively) are improved in the first scenario using BESS. considering no limitation in exchanged power,

TABLE 7. The effect of bess on total cost and MG reliability indices.

Scenario	Scenario 1- Without BESS	Scenario 1- With BESS	Changes %	Scenario 2- Without BESS	Scenario 2- With BESS	Changes %	Scenario 3- Without BESS	Scenario 3- With BESS	Changes %
Total Electricity Price (\$)- 24 hours	708.78	651.64	-8.06	703.63	701.69	-0.27	860.01	840.06	-2.31
LOLE (hr)	1.7092	0.7486	-56.20	0.7088	0.7098	0.14	0.8698	0.8457	-2.77
EENS (KWh)	70.9632	45.5739	-35.77	47.3580	45.2643	-4.42	59.5134	53.4402	-10.20

TABLE 8. The effect of bess types on total cost.

Scenario	MG Cost (\$):	MG Cost (\$):	MG Cost (\$):
	Scenario 1 – 23 KW	Scenario 2 – 23 KW	Scenario 3 – 65 KW
Lead-acid	651.64	701.69	849.47
NiCd / NiMH	691.79	723.59	861.21
Li-Ion	661.37	709.4	851.28
Sodium-Sulfur (NaS)	689.52	721.25	859.6
RFB / HFB	682.54	718.63	840.06

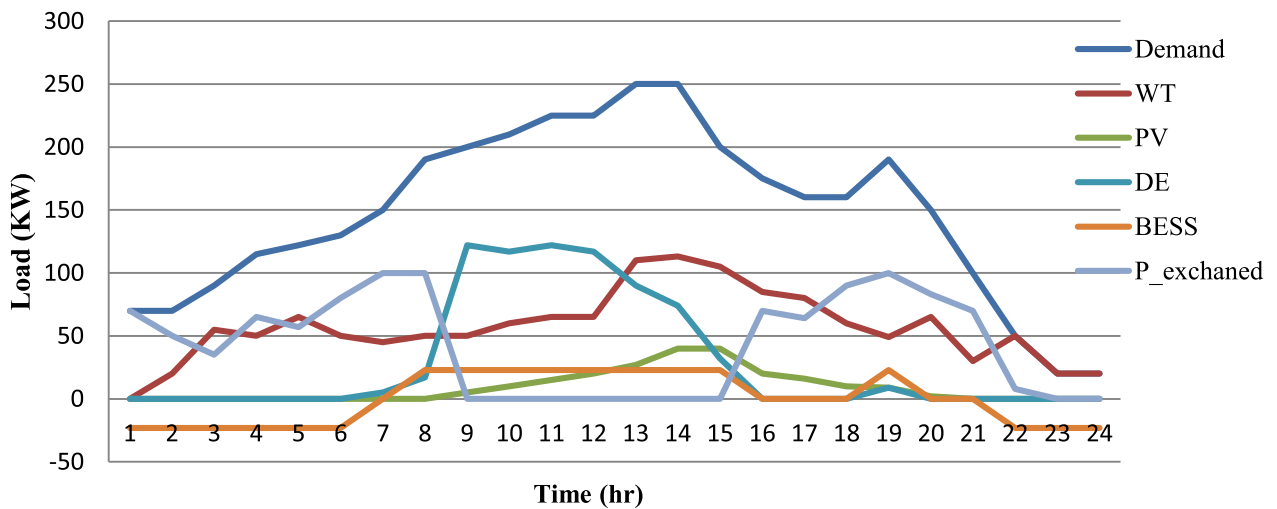


FIGURE 2. Energy distribution for the first scenario (grid-connected MG with limited exchanged power).

the second scenario, approximately, there is no improvement in total cost (just 0.27%) and reliability of MG (0.14% and 4.42% in LOLE and EENS) by using BESS. A 65 Kw RFB / HFB type, with the rated energy of 482 KWh, is the suggested BESS for the islanded MG. there is slight improvement in total cost, 2.31%, considering BESS. in addition, the LOLE and EENS are improved 2.77% and 10.2% respectively.

Moreover, the Table 8 provides the impact of different BESS types on the total cost of the MG. The results incorporate average values given in Table 2, considering the same size of BESS employed in each scenario. The results of Table 8 show the importance of selecting a proper type for BESS. After Lead-acid, The Li-Ion BESS type leads to lower total cost compare to other types. More discussion

regarding the achieved results is provided in the next section.

### V. DISCUSSION

In this section, we will discuss the achievements of the study as follows:

- Compared to other studies considering the effect of BESS on MG total cost and reliability, the results of this study have demonstrated acceptable improvements. In the case of grid-connected MG, we achieved up to a 56.2% reduction in the Loss of Load Expectation (LOLE) and a 35.77% reduction in the Expected Energy Not Supplied (EENS), resulting in a notable enhancement in reliability. Additionally, the total cost of the MG decreased by 8.06% in this scenario.

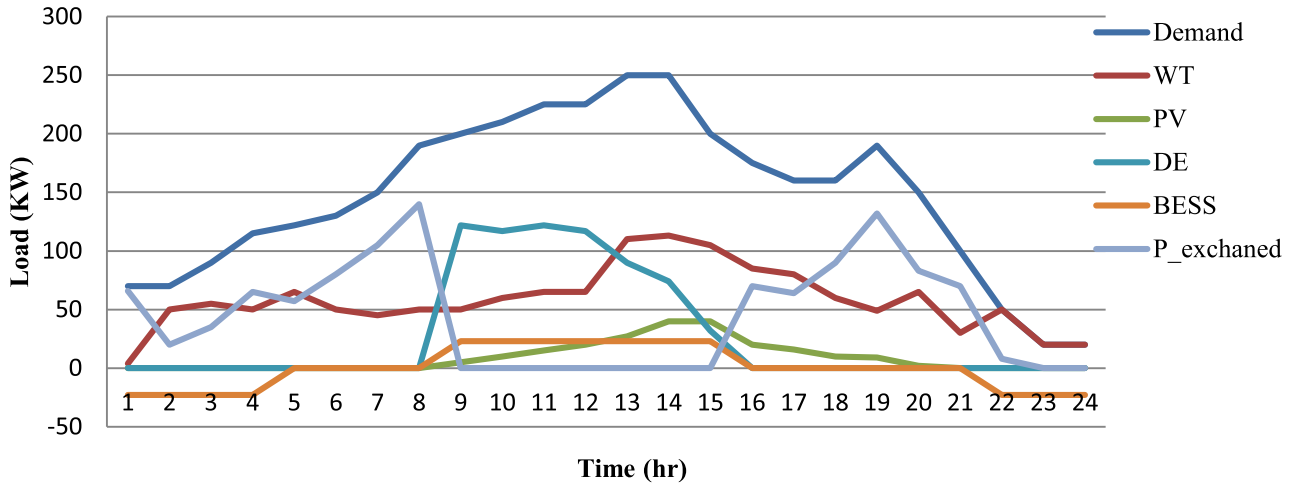


FIGURE 3. Energy distribution for the second scenario (grid-connected MG without limited exchanged power).

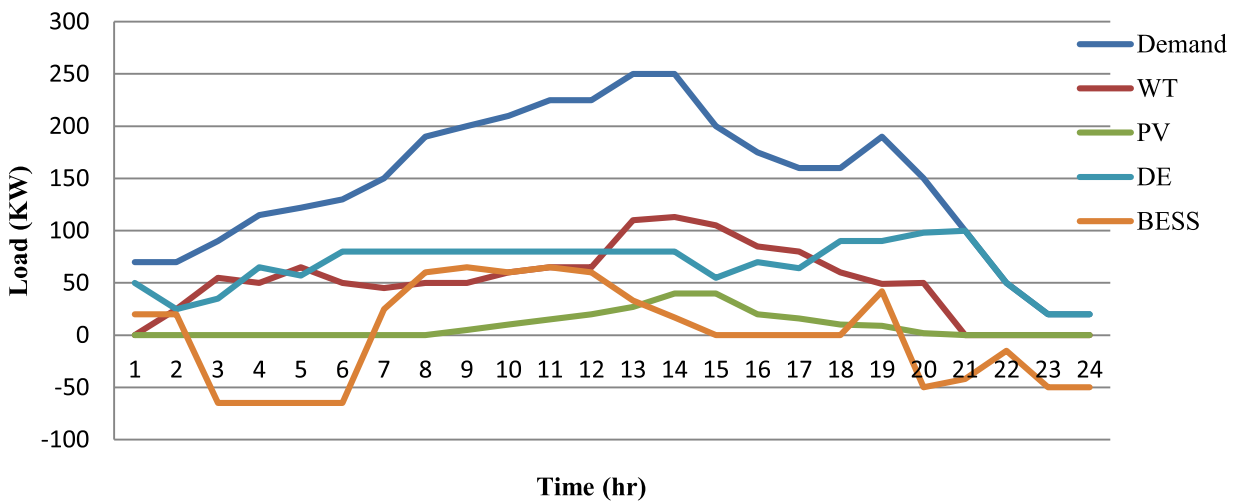


FIGURE 4. Energy distribution for the third scenario (islanded MG).

For reference [18], the study reported improvements of 19.56% and 36.05% in EENS by installing 2MWh and 5MWh mobile BESS, respectively. In reference [19], the total cost of the MG was reduced by 0.98%, accompanied by a 15% improvement in the Customer Average Interruption Duration (CAIDI) index as a reliability measure. Furthermore, the utilization of PV-BESS, WT-BESS, and PV-WT-BESS combinations in [32] led to substantial improvements in EENS, with enhancements of 37.43%, 33.9%, and 54.89% respectively.

- In grid-connected MGs with limitations in exchanged power with the main grid, lead-acid battery with a rated power of 23 KW and rated energy of 258 KWh is suggested. By utilizing BESS, both Loss of Load Expectation (LOLE) and Energy Not Supplied (EENS) can be improved by 56.20% and 35.77% respectively. The total cost can also be reduced by 8.06%. This is because BESS can be charged during off-peak and normal hours and discharged during peak hours, as expected.

- In the case of grid-connected MGs without limitations in exchanged power, there is no significant improvement in total cost (only 0.27%). Regarding reliability indices, there is a 0.14% increase in LOLE and a 4.42% decrease in EENS. Considering the installation and other costs, the total cost may even increase.

- For islanded MGs, the optimal solution is to use a 65 KW RFB/HFB type battery. Also, the rated energy found is to be 482 KWh which is remarkably higher than rated energy suggested for the grid-connected MG. This higher capacity is necessary because the load can only be supplied by PV, WT, DE, and BESS. The improvement in total cost and reliability is not significant, with only a 2.31% cost saving in islanded MGs. LOLE and EENS were decreased by 2.77% and 10.20%, respectively. Additionally, the results indicate that in the islanded MG scenario, the BESS is utilized to supply the load during both peak and normal hours. On the other hand, in other scenarios, the BESS is primarily used during peak hours. This distinction in usage patterns results

in a significantly higher number of charging and discharging cycles and overall hours of operation for the BESS in the islanded MG case compared to the grid-connected MG case. Consequently, the need for more frequent replacements and higher operational costs arises. Considering this perspective, it is suggested that BESS types with a higher number of lifecycles are more suitable for islanded MG applications. According to data provided in Table 2, RFB and HFB exhibit higher life cycles ranging from 12,000 to 14,000 compared to other BESS types.

- The results are highly sensitive to factors such as the price of electricity in different hours of the day, the total energy cost of BESS (\$/kWh), and the load profile, especially the load demand during peak hours. Therefore, the same study should be conducted for every specific case of study. Overall, the type of BESS and MG are important factors to consider when designing MGs. In cases where there is a possibility to exchange power with the main grid, and considering maintenance, installation, and space constraints of BESS, utilizing BESS may not be recommended. In addition, in islanded MGs, BESS types with a higher number of lifecycles, such as RFB and HFB, are deemed suitable based on their extended lifespan.

## VI. CONCLUSION

In conclusion, this study addressed the issue of finding the optimal size and type of battery energy storage systems (BESS) to improve the reliability of MGs. Several factors of the BESS, such as rated power, power cost, discharge time, efficiency, and life cycle, based on the type of ESS were considered. A particle swarm optimization algorithm was applied to determine the optimized size, with the total cost considered as the fitness function for the problem.

The study further suggests that the optimum size of BESS in grid-connected MGs is 23 KW, with the recommended type being Lead-acid. In contrast, due to the high number of charging and discharging cycles required in islanded MGs, it is better to use redox flow batteries (RFB) or hybrid flow batteries (HFB) types, which have a higher number of life cycles.

In summary, the study provides valuable insights for MG designers and operators in selecting the optimal size and type of BESS for their specific applications, while ensuring cost-effectiveness and reliability improvement. For future work, it would be interesting to investigate the feasibility and effectiveness of passive energy storage systems in MGs and compare their performance with battery energy storage systems. Passive energy storage systems have been gaining attention due to their potential advantages over BESS, including longer lifetimes, and faster response times. In addition to the future work mentioned above, it would be worthwhile to explore the optimal sizing of BESS while considering the multi-use approach and value-stacking such as peak shaving, frequency regulation, demand response, and renewable integration.

## REFERENCES

- [1] S. D'silva, M. Shadmand, S. Bayhan, and H. Abu-Rub, "Towards grid of microgrids: Seamless transition between grid-connected and islanded modes of operation," *IEEE Open J. Ind. Electron. Soc.*, vol. 1, pp. 66–81, 2020, doi: [10.1109/OJIES.2020.2988618](https://doi.org/10.1109/OJIES.2020.2988618).
- [2] N. Sharmila, K. R. Nataraj, and K. Rekha, "An overview on design and control schemes of microgrid," in *Proc. Global Conf. Advancement Technol. (GCAT)*, Oct. 2019, pp. 1–4, doi: [10.1109/GCAT47503.2019.8978407](https://doi.org/10.1109/GCAT47503.2019.8978407).
- [3] S. Impram, S. V. Nese, and B. Oral, "Challenges of renewable energy penetration on power system flexibility: A survey," *Energy Strategy Rev.*, vol. 31, Sep. 2020, Art. no. 100539, doi: [10.1016/j.esr.2020.100539](https://doi.org/10.1016/j.esr.2020.100539).
- [4] S. Bahramirad, W. Reder, and A. Khodaei, "Reliability-constrained optimal sizing of energy storage system in a microgrid," *IEEE Trans. Smart Grid*, vol. 3, no. 4, pp. 2056–2062, Dec. 2012, doi: [10.1109/TSG.2012.2217991](https://doi.org/10.1109/TSG.2012.2217991).
- [5] P. Buchana and T. S. Ustun, "The role of microgrids & renewable energy in addressing sub-Saharan Africa's current and future energy needs," in *Proc. IREC 6th Int. Renew. Energy Congr.*, Mar. 2015, pp. 1–6, doi: [10.1109/IREC.2015.7110977](https://doi.org/10.1109/IREC.2015.7110977).
- [6] IRENA. (2015). *From Baseload to Peak?: Renewables Provide a Reliable Solution*. [Online]. Available: [http://www.irena.org/DocumentDownloads/Publications/IRENA\\_Baseload\\_to\\_Peak\\_2015.pdf](http://www.irena.org/DocumentDownloads/Publications/IRENA_Baseload_to_Peak_2015.pdf)
- [7] Y. O. Shaker, D. Youfri, A. Osama, A. Al-Gindy, E. Tag-Eldin, and D. Allam, "Optimal charging/discharging decision of energy storage community in grid-connected microgrid using multi-objective hunger game search optimizer," *IEEE Access*, vol. 9, pp. 120774–120794, 2021, doi: [10.1109/ACCESS.2021.3101839](https://doi.org/10.1109/ACCESS.2021.3101839).
- [8] M. G. Al-Mufti and R. A. Ghani, "Control of battery energy storage system for peak shaving using enhanced time of use scheme," in *Proc. IEEE Int. Conf. Power Energy (PECon)*, Dec. 2020, pp. 224–228, doi: [10.1109/PECon48942.2020.9314416](https://doi.org/10.1109/PECon48942.2020.9314416).
- [9] C. K. Das, O. Bass, G. Kothapalli, T. S. Mahmoud, and D. Habibi, "Overview of energy storage systems in distribution networks: Placement, sizing, operation, and power quality," *Renew. Sustain. Energy Rev.*, vol. 91, pp. 1205–1230, Aug. 2018, doi: [10.1016/j.rser.2018.03.068](https://doi.org/10.1016/j.rser.2018.03.068).
- [10] H. Nazari-pouya, Y.-W. Chung, and A. Akhil, "Energy storage in microgrids: Challenges, applications and research need," *Int. J. Energy Smart Grid*, vol. 3, no. 2, pp. 60–70, Jul. 2019, doi: [10.23884/ijesg.2018.3.2.02](https://doi.org/10.23884/ijesg.2018.3.2.02).
- [11] S. X. Chen, H. B. Gooi, and M. Q. Wang, "Sizing of energy storage for microgrids," *IEEE Trans. Smart Grid*, vol. 3, no. 1, pp. 142–151, Mar. 2012, doi: [10.1109/TSG.2011.2160745](https://doi.org/10.1109/TSG.2011.2160745).
- [12] S. Bahramirad and E. Camm, "Practical modeling of smart grid SMS storage management system in a microgrid," in *Proc. PES T&D*, May 2012, pp. 1–7, doi: [10.1109/TDC.2012.6281697](https://doi.org/10.1109/TDC.2012.6281697).
- [13] P. P. Gupta, P. Jain, S. Sharma, and R. Bhakar, "Reliability-security constrained unit commitment based on benders decomposition and mixed integer non-linear programming," in *Proc. Int. Conf. Comput., Commun. Electron. (Comptelx)*, Jul. 2017, pp. 328–333, doi: [10.1109/COMPTELIX.2017.8003988](https://doi.org/10.1109/COMPTELIX.2017.8003988).
- [14] T. A. Nguyen, M. L. Crow, and A. C. Elmore, "Optimal sizing of a vanadium redox battery system for microgrid systems," *IEEE Trans. Sustain. Energy*, vol. 6, no. 3, pp. 729–737, Jul. 2015, doi: [10.1109/TSTE.2015.2404780](https://doi.org/10.1109/TSTE.2015.2404780).
- [15] N. T. Mbungu, R. Naidoo, R. C. Bansal, and M. Bipath, "Optimisation of grid connected hybrid photovoltaic-wind-battery system using model predictive control design," *IET Renew. Power Gener.*, vol. 11, no. 14, pp. 1760–1768, Dec. 2017, doi: [10.1049/iet-rpg.2017.0381](https://doi.org/10.1049/iet-rpg.2017.0381).
- [16] P. Xiong, P. Jirutitijaroen, and C. Singh, "A distributionally robust optimization model for unit commitment considering uncertain wind power generation," *IEEE Trans. Power Syst.*, vol. 32, no. 1, pp. 39–49, Jan. 2017, doi: [10.1109/TPWRS.2016.2544795](https://doi.org/10.1109/TPWRS.2016.2544795).
- [17] N. Nikmehr and S. Najafi-Ravadanegh, "Optimal operation of distributed generations in micro-grids under uncertainties in load and renewable power generation using heuristic algorithm," *IET Renew. Power Gener.*, vol. 9, no. 8, pp. 982–990, Nov. 2015, doi: [10.1049/iet-rpg.2014.0357](https://doi.org/10.1049/iet-rpg.2014.0357).
- [18] Y. Chen, Y. Zheng, F. Luo, J. Wen, and Z. Xu, "Reliability evaluation of distribution systems with mobile energy storage systems," *IET Renew. Power Gener.*, vol. 10, no. 10, pp. 1562–1569, Nov. 2016, doi: [10.1049/iet-rpg.2015.0608](https://doi.org/10.1049/iet-rpg.2015.0608).
- [19] M. A. Abdulgalil and M. Khalid, "Enhancing the reliability of a microgrid through optimal size of battery ESS," *IET Gener., Transmiss. Distrib.*, vol. 13, no. 9, pp. 1499–1508, May 2019, doi: [10.1049/iet-gtd.2018.5335](https://doi.org/10.1049/iet-gtd.2018.5335).

- [20] B. Steffen, "Prospects for pumped-hydro storage in Germany," *Energy Policy*, vol. 45, pp. 420–429, Jun. 2012, doi: [10.1016/j.enpol.2012.02.052](https://doi.org/10.1016/j.enpol.2012.02.052).
- [21] C. Krupke, J. Wang, J. Clarke, and X. Luo, "Modeling and experimental study of a wind turbine system in hybrid connection with compressed air energy storage," *IEEE Trans. Energy Convers.*, vol. 32, no. 1, pp. 137–145, Mar. 2017, doi: [10.1109/TEC.2016.2594285](https://doi.org/10.1109/TEC.2016.2594285).
- [22] M. I. Daoud, A. M. Massoud, A. S. Abdel-Khalik, A. Elserougi, and S. Ahmed, "A flywheel energy storage system for fault ride through support of grid-connected VSC HVDC-based offshore wind farms," *IEEE Trans. Power Syst.*, vol. 31, no. 3, pp. 1671–1680, May 2016, doi: [10.1109/TPWRS.2015.2465163](https://doi.org/10.1109/TPWRS.2015.2465163).
- [23] A. M. Gee, F. Robinson, and W. Yuan, "A superconducting magnetic energy storage-emulator/battery supported dynamic voltage restorer," *IEEE Trans. Energy Convers.*, vol. 32, no. 1, pp. 55–64, Mar. 2017, doi: [10.1109/TEC.2016.2609403](https://doi.org/10.1109/TEC.2016.2609403).
- [24] X. Chang, Y. Li, X. Li, and X. Chen, "An active damping method based on a supercapacitor energy storage system to overcome the destabilizing effect of instantaneous constant power loads in DC microgrids," *IEEE Trans. Energy Convers.*, vol. 32, no. 1, pp. 36–47, Mar. 2017, doi: [10.1109/TEC.2016.2605764](https://doi.org/10.1109/TEC.2016.2605764).
- [25] M. R. Chakraborty, S. Dawn, P. K. Saha, J. B. Basu, and T. S. Ustun, "A comparative review on energy storage systems and their application in deregulated systems," *Batteries*, vol. 8, no. 9, p. 124, Sep. 2022, doi: [10.3390/batteries8090124](https://doi.org/10.3390/batteries8090124).
- [26] E. M. G. Rodrigues, G. J. Osório, R. Godina, A. W. Bizuayehu, J. M. Lujano-Rojas, J. C. O. Matias, and J. P. S. Catalão, "Modelling and sizing of NaS (sodium sulfur) battery energy storage system for extending wind power performance in Crete Island," *Energy*, vol. 90, pp. 1606–1617, Oct. 2015, doi: [10.1016/j.energy.2015.06.116](https://doi.org/10.1016/j.energy.2015.06.116).
- [27] M. K. Ravikumar, S. Rathod, N. Jaiswal, S. Patil, and A. Shukla, "The renaissance in redox flow batteries," *J. Solid State Electrochem.*, vol. 21, no. 9, pp. 2467–2488, Sep. 2017, doi: [10.1007/s10008-016-3472-4](https://doi.org/10.1007/s10008-016-3472-4).
- [28] T. Nguyen-Duc, L. Hoang-Tuan, H. Ta-Xuan, L. Do-Van, and H. Takano, "A mixed-integer programming approach for unit commitment in microgrid with incentive-based demand response and battery energy storage system," *Energies*, vol. 15, no. 19, p. 7192, Sep. 2022, doi: [10.3390/en15197192](https://doi.org/10.3390/en15197192).
- [29] J. Moore and B. Shabani, "A critical study of stationary energy storage policies in Australia in an international context: The role of hydrogen and battery technologies," *Energies*, vol. 9, no. 9, p. 674, Aug. 2016, doi: [10.3390/en9090674](https://doi.org/10.3390/en9090674).
- [30] G. Kucur, M. R. Tur, R. Bayindir, H. Shahinzadeh, and G. B. Gharehpetian, "A review of emerging cutting-edge energy storage technologies for smart grids purposes," in *Proc. 9th Iranian Conf. Renew. Energy Distrib. Gener. (ICREDG)*, Feb. 2022, pp. 1–11, doi: [10.1109/ICREDG54199.2022.9804538](https://doi.org/10.1109/ICREDG54199.2022.9804538).
- [31] M. Aslani, H. Hashemi-Dezaki, and A. Ketabi, "Reliability evaluation of smart microgrids considering cyber failures and disturbances under various cyber network topologies and distributed Generation's scenarios," *Sustainability*, vol. 13, no. 10, p. 5695, May 2021, doi: [10.3390/su13105695](https://doi.org/10.3390/su13105695).
- [32] T. Adefarati and R. C. Bansal, "Reliability and economic assessment of a microgrid power system with the integration of renewable energy resources," *Appl. Energy*, vol. 206, pp. 911–933, Nov. 2017, doi: [10.1016/j.apenergy.2017.08.228](https://doi.org/10.1016/j.apenergy.2017.08.228).



**MOHAMMADREZA GHOLAMI** was born in Hamedan, Iran. He received the B.S. degree in electrical engineering from Bu-Ali Sina University, in 2006, and the M.S. degree in electrical engineering from Zanjan University, in 2008. He is currently an Instructor with the Department of Electrical Engineering, Final International University. His research interests include power systems and smart grids reliability and the application of optimization methods.



**SOAD ABOKHAMIS MOUSAVI** received the B.A. degree from the Islamic Azad University of Dezful, in 2008, the M.A. degree from the Department of Architecture, Islamic Azad University of Shoushtar, in 2010, and the Ph.D. degree from the Department of Architecture, Eastern Mediterranean University, in 2018. She is currently the Vice Dean and a Faculty Member of the Department of Architecture, Final International University. Her research interests include sustainability, climate change, and energy.



**S. M. MUYEEN** (Senior Member, IEEE) received the B.Sc. degree in electrical and electronic engineering from the Rajshahi University of Engineering and Technology (RUET, formerly known as the Rajshahi Institute of Technology), Bangladesh, in 2000, and the M.Eng. and Ph.D. degrees in electrical and electronic engineering from the Kitami Institute of Technology, Japan, in 2005 and 2008, respectively. He is currently a Full Professor with the Department of Electrical Engineering, Qatar University. He has published more than 250 papers in different journals and international conferences. He has also published seven books as the author or an editor. His research interests include power system stability and control, electrical machine, FACTS, energy storage systems (ESSs), renewable energy, and HVDC systems. He is a fellow of Engineers Australia. He is serving as an Editor/Associate Editor for many prestigious journals, such as IEEE, IET, and other publishers, including IEEE TRANSACTIONS ON ENERGY CONVERSION, IEEE POWER ENGINEERING LETTERS, *IET Renewable Power Generation*, and *IET Generation, Transmission and Distribution*. He has been a keynote speaker and an invited speaker at many international conferences, workshops, and universities.

• • •